Kikuchi-Fujimoto Disease

PET/CT Assessment of a Rare Cause of Cervical Lymphadenopathy

Tetsuya Tsujikawa, MD, PhD, Tatsuro Tsuchida, MD, PhD,* Yoshiaki Imamura, MD, PhD,† Masato Kobayashi, PhD,‡ Satoko Asahi, MD,* Kazuhiro Shimizu, MD,* Kazunobu Tsuji, MD,* Hidehiko Okazawa, MD, PhD,§ and Hirohiko Kimura, MD, PhD**

Purpose: Kikuchi-Fujimoto disease (KFD), formerly called subacute necrotizing lymphadenitis, is a rare cause of cervical lymphadenopathy. The purpose of this study was to evaluate the usefulness of FDG PET/CT for distinguishing KFD from non-Hodgkin lymphoma (NHL).

Materials and Methods: Twenty-two patients with cervical lymphadenopathy (8 with KFD and 14 with NHL) underwent CT and FDG PET/CT scans to examine the cervical lymphadenopathy. Regional values of FDG uptake were evaluated using the standardized uptake value (SUV) and partial volume corrected SUV ($_{cor}$SUV) based on the count recovery coefficient. Tumor size (mm), SUV, and $_{cor}$SUV were compared among KFD, indolent NHL, and aggressive NHL.

Results: KFD lesions tended to be smaller (13.8 ± 5.4 mm) than those of indolent (25.4 ± 11.8) and aggressive (29.7 ± 18.8) NHL, whereas there were no significant differences in size. As for SUV, a significant difference was observed only between indolent and aggressive (6.4 ± 1.5 and 17.3 ± 9.3, $P < 0.05$) NHL; however, KFD showed a significantly greater $_{cor}$SUV (23.8 ± 10.6) as compared with indolent NHL (9.2 ± 5.1, $P < 0.05$), which did not show a significant difference from aggressive NHL (21.4 ± 10.2). FDG PET/CT detected thoracoabdominal lesions in 2 patients (25%) with KFD.

Conclusions: KFD shows high FDG uptake for size, which may reflect the pathologic characteristics, including necrotizing lymphocytes and numerous histiocytes (macrophages) surrounding small necrotic foci. FDG PET/CT will be useful for detecting noncervical lesions of KFD and distinguishing KFD from NHLs using both SUV and $_{cor}$SUV.

Key Words: Kikuchi-Fujimoto disease, FDG, PET/CT

(*Clin Nucl Med* 2011;36: 661–664)

Kikuchi-Fujimoto disease (KFD) or histiocytic necrotizing lymphadenitis, formerly called subacute necrotizing lymphadenitis, is a self-limiting cause of cervical lymphadenopathy. First described independently in 1972 by Kikuchi and Fujimoto et al,[1,2] KFD is an extremely rare disease known to have a worldwide distribution with higher prevalence among Japanese and other Asiatic individuals.[3]

Characteristic histopathologic features of KFD include variable degrees of necrosis in cortical and paracortical areas with abundant karyorrhectic debris, numerous histiocytes at the margin of the necrotic areas, and the absence of granulocytes[4,5]; however, despite the histopathologic features of KFD, previous studies have reported that most lymph nodes were homogeneously enhanced without evidence of gross necrosis on computed tomography (CT).[6–8] Several case reports and a recent study using positron emission tomography (PET) with 2-[F-18]fluoro-2-deoxy-D-glucose (FDG) have suggested that the lymph nodes of patients with KFD exhibit FDG avidity[9–13]; that is, CT and FDG PET findings of KFD mimic those of malignant lymphoma.

On the other hand, it is reported that affected lymph nodes in KFD are not very large (diameter of <3–3.5 cm).[6,13] Because the partial volume effect (PVE) is one of the most important factors affecting FDG uptake on PET imaging,[14,15] the purpose of this study was to evaluate the usefulness of FDG PET/CT to distinguish among KFD, indolent non-Hodgkin lymphoma (NHL) and aggressive NHL using regional FDG uptake with and without partial volume correction. In addition, we described the histopathologic correlation with PET imaging features of KFD.

MATERIALS AND METHODS

Patients

A search of our institution's pathology, radiology, and medical records between November 2006 and March 2010 revealed 8 patients with KFD and 14 patients with NHL (5 indolent and 9 aggressive) whose data were considered for inclusion in this retrospective study. Patient data were included if they were referred to our institution for examination of cervical lymphadenopathy with or without fever, if they had a pathologically proven diagnosis of KFD or NHL by excisional biopsy from cervical lymph nodes, and if they had undergone both CT and FDG PET/CT at the time of diagnosis. Exclusion criteria were as follows: lack of pathologic diagnosis, main affected area other than cervical nodes.

CT and PET/CT Imaging

Eighteen CT examinations of the neck were performed with a multidetector CT scanner with 16 detectors (LightSpeed Ultra; GE Medical Systems, Milwaukee, WI) before and after intravenous administration of nonionic iodinated contrast material (iopamidol, Iopamiron 300; Schering, Berlin, Germany). Three CT examinations were performed without contrast material. The CT parameters were as follows: peak tube voltage of 120 to 400 mAs, rotation time of 0.5 seconds, reconstruction thickness of 5 mm, pitch of 8, and with 16-row detector configuration.

All whole-body PET scans with FDG were performed with a combined PET/CT scanner (Discovery LS; GE Medical Systems), which permits simultaneous acquisition of 35 image slices in 3-dimensional acquisition mode with interslice spacing of 4.25 mm. The PET/CT scanner incorporates an integrated 4-slice multidetector CT scanner, which was used for attenuation correction. CT scanning parameters were as follows: Auto mA (upper limit, 40 mA; noise index, 20), 140 kV, 5-mm section thickness, 15-mm table feed, and pitch of 4. After at least 4 hours fasting, patients received an intravenous injection of 185 MBq FDG and image acquisition began 50 minutes after injection. A whole-body emission scan was performed from the head to the inguinal region with 2 minutes per bed

Received for publication December 22, 2010; revision accepted February 14, 2011.
From the *Department of Radiology, University of Fukui, Fukui, Japan; †Division of Surgical Pathology, University of Fukui, Fukui, Japan; ‡School of Health Sciences, College of Medical, Pharmaceutical and Health Sciences, Kanazawa University, Kanazawa, Japan; and §Biomedical Imaging Research Center, University of Fukui, Fukui, Japan.

Reprints: Tetsuya Tsujikawa, MD, PhD, Department of Radiology, University of Fukui, 23–3 Matsuoka-Shimoaizuki, Eiheiji-cho, Fukui 910–1193, Japan. E-mail: awaji@u-fukui.ac.jp.

ISSN: 0363-9762/11/3608-0661

position (7 to 8 bed positions). PET data were reconstructed by the iterative reconstruction method selecting 14 subsets and 2 iterations. The reconstructed images were then converted to a semiquantitative image corrected by the injection dose and subject's body weight (= standardized uptake value [SUV]).

Phantom Study

NEMA 2001 body phantom, which is an elliptical phantom with 6 individually fillable spheres whose diameters range from 10, 13, 17, 22, 28, and 37 mm, was prepared. The concentration of F-18 FDG in all the spheres was 10 kBq/mL and lowest lesser one in the background was 2 kBq/mL. The PET/CT system and imaging protocol were the same as the clinical scan except that the emission scan was obtained for 5 minutes. Circular regions of interest (ROIs) were placed over the surface with the greatest diameter of each hot sphere on the image, and the ROI of the hot sphere invisible on the image was located using the corresponding CT image. The relative recovery coefficient (RC) was calculated using the following formula:

$$RC = A/B,$$

where A is the maximum pixel count of each hot sphere and B is the maximum pixel count of the greatest sphere without PVE.

The regression count recovery curve was obtained and used for further analysis.

Image Analysis

For PET/CT image analysis, single ROIs as large as possible were placed over the cervical lymph node showing the highest FDG uptake using information obtained from CT images by the consensus of 2 experienced nuclear medicine physicians. SUV was determined as the highest activity within an ROI and the maximum diameter of the lymph node was recorded per patient. RC of the lesion was determined using the regression curve. Partial volume corrected SUV ($_{cor}$SUV) was calculated as[16–18]:

$$_{cor}SUV = (SUV - {}_{back}SUV)/RC + {}_{back}SUV,$$

where $_{back}$SUV denotes SUV of background (cervical muscles).

Statistical Analysis

All patients were divided into 3 groups consisting of KFD, indolent NHL, and aggressive NHL. Tumor size (mm), SUV, and $_{cor}$SUV were compared among the 3 groups by 1-way ANOVA with a post hoc Games-Howell test, which has robustness for analysis even in unequal variance. A probability value of less than 0.05 was considered to indicate significant difference. Statistical analysis was performed using a software package (PASW Statistics, formerly called SPSS Statistics, 17.0; SPSS Inc).

RESULTS

Figure 1 shows that the lesions of KFD had a tendency to be smaller (13.8 ± 5.4 mm) than those of indolent NHL (25.4 ± 11.8) and aggressive NHL (29.7 ± 18.8), whereas there were no significant differences in size. As for SUV, a significant difference was observed only between indolent NHL and aggressive NHL (6.4 ± 1.5 and 17.3 ± 9.3, $P < 0.05$). On the other hand, KFD showed a significantly greater $_{cor}$SUV (23.8 ± 10.6) than indolent NHL (9.2 ± 5.1, $P < 0.05$), which did not show a significant difference from aggressive NHL (21.4 ± 10.2).

Six patients had homogeneous lymph nodes on CT images. Affected nodes contained low-attenuation areas suggesting gross nodal necrosis in 2 cases (25%). A representative case of a 16-year-old boy with histopathologic findings is given in Figure 2. FDG PET/CT showed intense accumulation of FDG on right cervical lymphadenopathy (Fig. 2A). A CT scan showed multiple small and medium homogenously enhanced nodes without evidence of gross necrosis (Fig. 2B). Despite the CT findings, histologically, a lymph node showed a well-circumscribed paracortical focus of necrosis with a mixture of karyorrhectic nuclear debris, single cell necrosis, transformed lymphocytes, and foamy histiocytes (macrophages). Polymorphonuclear leukocytes were absent (Figs. 2C, D).

Whole-body PET/CT detected thoracoabdominal lesions in 2 patients with KFD. In one of the patients, affected lymph nodes along the celiac artery were first noted on whole-body PET/CT (Figs. 3C–E), not on nonenhanced abdominal CT (not shown).

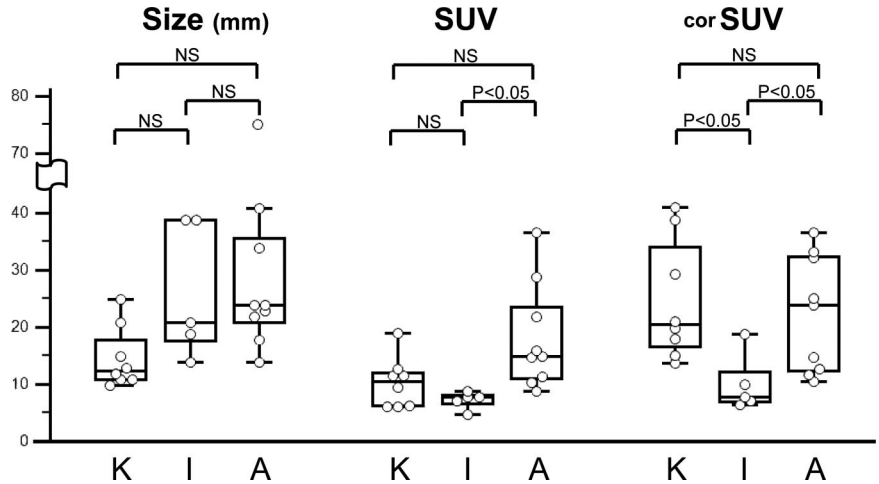

FIGURE 1. Box-and-whisker plots of each lesion size, FDG uptake (SUV), and partial volume corrected FDG uptake ($_{cor}$SUV) among KFD, indolent NHL, and aggressive NHL. KFD had a tendency to be smaller (13.8 ± 5.4 mm) than those of indolent NHL (25.4 ± 11.8) and aggressive NHL (29.7 ± 18.8), whereas there were no significant differences in size among them. As for SUV, a significant difference was observed only between indolent NHL and aggressive NHL (6.4 ± 1.5 and 17.3 ± 9.3, $P < 0.05$). On the other hand, KFD showed a significantly greater $_{cor}$SUV (23.8 ± 10.6) than those of indolent NHL (9.2 ± 5.1, $P < 0.05$), which did not show a significant difference from aggressive NHL (21.4 ± 10.2). K indicates Kikuchi-Fujimoto disease; I, indolent NHL; A, aggressive NHL.

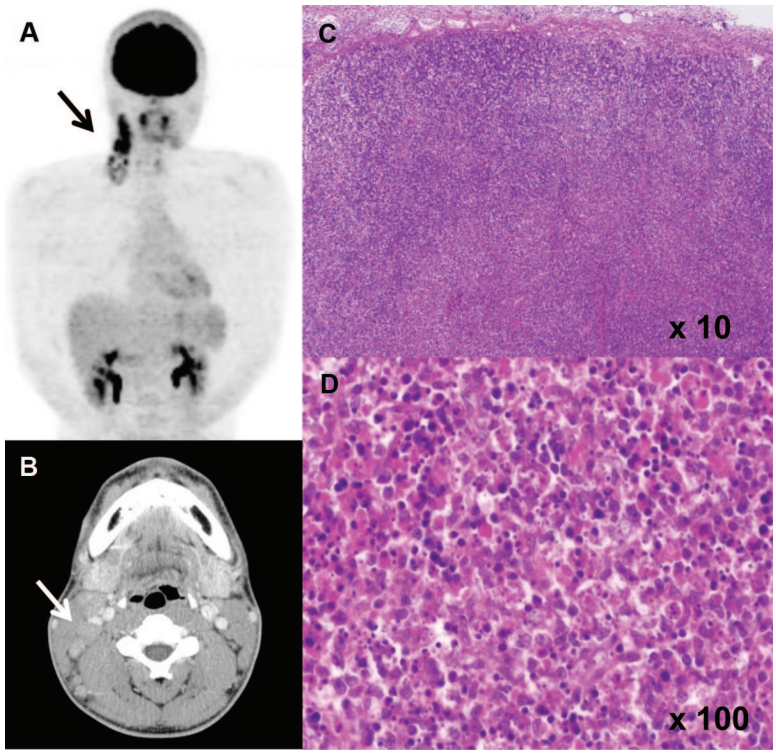

FIGURE 2. A 16-year-old male patient with KFD. Maximum intensity projection image of FDG PET/CT (**A**) shows intense accumulation of FDG in right cervical lymphadenopathy (arrow). Neck CT scan with contrast enhancement (**B**) shows multiple small and medium homogenously enhanced nodes without evidence of gross necrosis (arrow). Histologic images of right cervical lymph node on hematoxylin-eosin (**C, D**) show a well-circumscribed paracortical focus of necrosis with a mixture of karyorrhectic nuclear debris, single cell necrosis, transformed lymphocytes, and foamy histiocytes (macrophages). Polymorphonuclear leukocytes are absent.

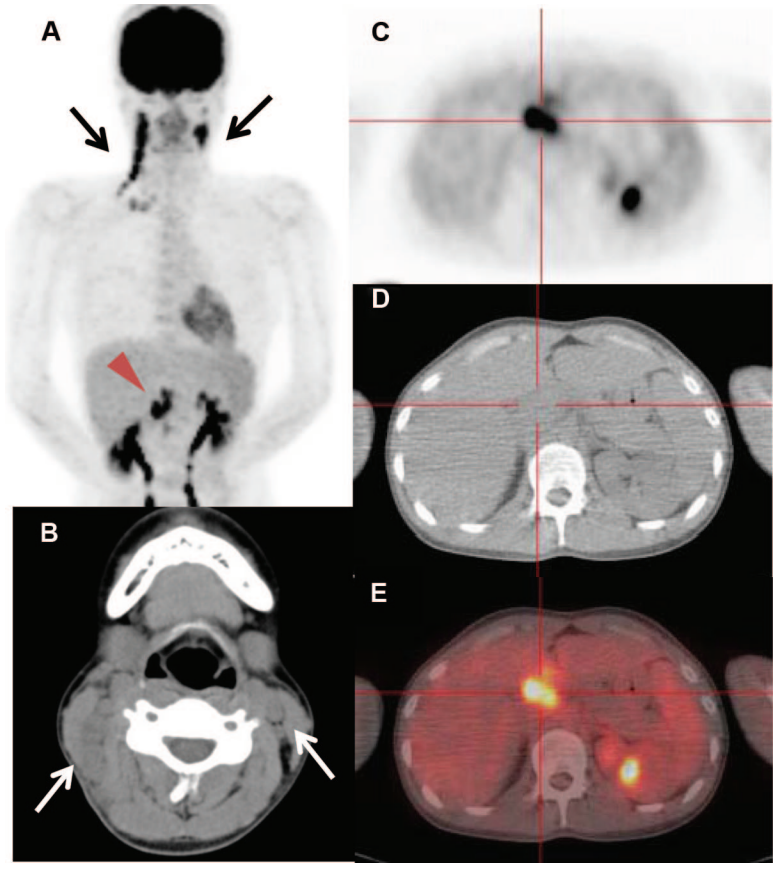

FIGURE 3. A 26-year-old female patient with KFD. Maximum intensity projection image of FDG PET/CT (**A**) shows intense accumulation of FDG in bilateral cervical, right supraclavicular (arrows), and abdominal lymphadenopathy (red arrowhead). Neck CT scan without contrast enhancement (**B**) shows multiple bilateral cervical lymphadenopathy (arrows). Affected lymph nodes along the celiac artery were first noted on whole-body PET/CT (**C–E**), not on nonenhanced abdominal CT (not shown).

DISCUSSION

KFD is a self-limiting cause of cervical lymphadenopathy, especially in young Asians, and it was previously reported to mimic malignant lymphoma on diagnostic imaging, such as CT and FDG PET.[6–13] On the other hand, several recent investigations described FDG uptake as being useful in differentiating different subgroups of lymphoma, that is, being lower in indolent than in aggressive lymphoma.[19–21] This study revealed that affected lymph nodes in patients with KFD had a tendency to be smaller than those of NHL; however, FDG uptake with partial volume correction ($_{cor}$SUV) of nodes in patients with KFD was higher than that of indolent NHL and almost the same as that of aggressive NHL. These results indicate that affected nodes of KFD show high FDG uptake for their size, which is expected to be a result of small necrotic foci and a collection of histiocytes (macrophages) in affected lymph nodes. Necrotic foci themselves should not show FDG accumulation, but necrotizing lymphocytes and numerous histiocytes (macrophages) surrounding small necrotic foci are expected to show intense FDG uptake. Since it is assumed that FDG uptake in inflammatory tissue is due to accumulation in inflammatory cells, such as macrophages,[22,23] lymphocytes,[24] and granulocytes,[25] in KFD macrophages and lymphocytes can cause high FDG avidity. Thus, when diagnosing FDG-avid small lymphadenopathy in young patients, KFD should be considered in the differential diagnosis. Additional $_{cor}$SUV measurement can be useful for revealing the pathologic features of KFD.

In addition to the degree of tracer uptake, FDG PET/CT was very useful for determining the extent of the disease. One-fourth of patients with KFD in this study (2 cases) had noncervical lesions, in one of which abdominal lymphadenopathy could be detected only by PET/CT. These results showed the same tendency as aggressive lymphoma. The use of PET/CT is likely to detect more noncervical lesions of KFD than ever before; however, the detection of thoracoabdominal lesions may confuse the diagnosis of KFD with that of stage of $\geq$2 lymphoma. We should be sensitive when diagnosing systemic lymphadenopathy in young patients, and consider the degree of lesion FDG uptake for size.

There are several limitations of this study. Hot spheres (10 kBq/mL) with a warm background (2 kBq/mL) when considering clinical cases were used for determining RC; however, in the human body, the ratio of a tumor to background activity in surrounding tissue varies according to its location. In addition, geometric factors and the heterogeneity of the lesions seemed to influence RC. Although it is difficult to compensate for PVE entirely on clinical PET imaging, the PET/CT system should be improved, and imaging and analysis protocols should be standardized to further reduce PVE and for more appropriate quantification of FDG PET studies in the future.

CONCLUSION

Affected lymph nodes of KFD show high FDG uptake for size, which may reflect the pathologic characteristics, including small necrotic areas and a collection of histiocytes. FDG PET/CT will be useful for detecting noncervical lesions of KFD and distinguishing KFD from NHLs using both SUV and $_{cor}$SUV.

REFERENCES

1. Kikuchi M. Lymphadenitis showing focal reticulum cell hyperplasia with nuclear debris and phagocytes: a clinicopathological study. *Acta Hematol Jpn*. 1972;35:379–380.
2. Fujimoto Y, Kozima Y, Yamaguchi K. Cervical subacute necrotizing lymphadenitis: a new clinicopathologic entity. *Naika*. 1972;20:920–927.
3. Mosharraf-Hossain AK, Datta PG, Amin AS, et al. Kikuchi-Fujimoto disease presenting with fever, lymphadenopathy and dysphagia. *J Pak Med Assoc*. 2008;58:647–649.
4. Dorfman RF, Berry GJ. Kikuchi's histiocytic necrotizing lymphadenitis: an analysis of 108 cases with emphasis on differential diagnosis. *Semin Diagn Pathol*. 1988;5:329–345.
5. Kuo TT. Kikuchi's disease (histiocytic necrotizing lymphadenitis). A clinicopathologic study of 79 cases with an analysis of histologic subtypes, immunohistology, and DNA ploidy. *Am J Surg Pathol*. 1995;19:798–809.
6. Kwon SY, Kim TK, Kim YS, et al. CT findings in Kikuchi disease: analysis of 96 cases. *Am J Neuroradiol*. 2004;25:1099–1102.
7. Na DG, Chung TS, Byun HS, et al. Kikuchi disease: CT and MR findings. *Am J Neuroradiol*. 1997;18:1729–1732.
8. Miller WT Jr, Perez-Jaffe LA. Cross-sectional imaging of Kikuchi disease. *J Comput Assist Tomogr*. 1999;23:548–551.
9. Liao AC, Chen YK. Cervical lymphadenopathy caused by Kikuchi disease: positron emission tomographic appearance. *Clin Nucl Med*. 2003;28:320–321.
10. Kim CH, Hyun OJ, Yoo IeR, et al. Kikuchi disease mimicking malignant lymphoma on FDG PET/CT. *Clin Nucl Med*. 2007;32:711–712.
11. Ito K, Morooka M, Kubota K. F-18 FDG PET/CT findings showing lymph node uptake in patients with Kikuchi disease. *Clin Nucl Med*. 2009;34:821–822.
12. Kaicker S, Gerard PS, Kalburgi S, et al. PET-CT scan in a patient with Kikuchi disease. *Pediatr Radiol*. 2008;38:596–597.
13. Ito K, Morooka M, Kubota K. Kikuchi disease: ^{18}F-FDG positron emission tomography/computed tomography of lymph node uptake. *Jpn J Radiol*. 2010;28:15–19.
14. Keyes JW Jr. SUV: standard uptake or silly useless value? *J Nucl Med*. 1995;36:1836–1839.
15. Geworski L, Knoop BO, de Cabrejas ML, et al. Recovery correction for quantitation in emission tomography: a feasibility study. *Eur J Nucl Med*. 2000;27:161–169.
16. Vesselle H, Schmidt RA, Pugsley JM, et al. Lung cancer proliferation correlates with [F-18]fluorodeoxyglucose uptake by positron emission tomography. *Clin Cancer Res*. 2000;6:3837–3844.
17. Vesselle H, Grierson J, Muzi M, et al. In vivo validation of 3′deoxy-3′-[^{18}F]fluorothymidine ([^{18}F]FLT) as a proliferation imaging tracer in humans: correlation of [^{18}F]FLT uptake by positron emission tomography with Ki-67 immunohistochemistry and flow cytometry in human lung tumors. *Clin Cancer Res*. 2002;8:3315–3323.
18. Degirmenci B, Wilson D, Laymon CM, et al. Standardized uptake value-based evaluations of solitary pulmonary nodules using F-18 fluorodeoxyglucose-PET/computed tomography. *Nucl Med Commun*. 2008;29:614–622.
19. Schoder H, Noy A, Gonen M, et al. Intensity of ^{18}Fluorodeoxyglucose uptake in positron emission tomography distinguishes between indolent and aggressive non-Hodgkin's lymphoma. *J Clin Oncol*. 2005;23:4643–4651.
20. Tsujikawa T, Otsuka H, Morita N, et al. Does partial volume corrected maximum SUV based on count recovery coefficient in 3D-PET/CT correlate with clinical aggressiveness of non-Hodgkin's lymphoma? *Ann Nucl Med*. 2008;22:23–30.
21. Ngeow JY, Quek RH, Ng DC, et al. High SUV uptake on FDG-PET/CT predicts for an aggressive B-cell lymphoma in a prospective study of primary FDG-PET/CT staging in lymphoma. *Ann Oncol*. 2009;20:1543–1547.
22. Defawe OD, Hustinx R, Defraigne JO, et al. Distribution of F-18 fluorodeoxyglucose (F-18 FDG) in abdominal aortic aneurysm: high accumulation in macrophages seen on PET imaging and immunohistology. *Clin Nucl Med*. 2005;30:340–341.
23. Kubota R, Yamada S, Kubota K, et al. Intratumoral distribution of fluorine-18-fluorodeoxyglucose in vivo: high accumulation in macrophages and granulation tissues studied by microautoradiography. *J Nucl Med*. 1992;33:1972–1980.
24. Ishimori T, Saga T, Mamede M, et al. Increased (18)F-FDG uptake in a model of inflammation: concanavalin A-mediated lymphocyte activation. *J Nucl Med*. 2002;43:658–663.
25. Jones HA, Cadwalladar KA, White JF, et al. Dissociation between respiratory burst activity and deoxyglucose uptake in human neutrophil granulocytes: implications for interpretation of 18F-FDG PET images. *J Nucl Med*. 2002;43:652–657.